JOURNAL OF MAGNETIC RESONANCE IMAGING 31:1355–1363 (2010)

Original Research

Late Stimulation of the Sphenopalatine-Ganglion in Ischemic Rats: Improvement in N-Acetyl-Aspartate Levels and Diffusion Weighted Imaging Characteristics as Seen by MR

Amnon Bar-Shir, MSc, Noam Shemesh, BSc, Revital Nossin-Manor, PhD,† and Yoram Cohen, PhD*

Purpose: To assess, by MR spectroscopy (MRS) and diffusion weighted imaging (DWI), the ability of electrical stimulation of the sphenopalatine ganglion (SPG) to augment stroke recovery in transient middle cerebral artery occluded (t-MCAO) rats, when treatment is started 18 ± 2 h post-occlusion.

Materials and Methods: ^{1}H-MRS imaging (^{1}H-MRSI) and DWI were used to evaluate ischemic brain tissue after SPG stimulation in rats subjected to 2 h of t-MCAO. Rats were examined by ^{1}H-MRSI, DWI, and behavioral tests at 16 ± 2 h, 8 days, and 28 days post-MCAO.

Results: N-Acetyl-aspartate (NAA) levels of the stimulated and control rats were the same 16 ± 2 h post-MCAO (0.52 ± 0.03, 0.54 ± 0.03). At 28 days post-occlusion, NAA levels were significantly higher in the treated group (0.60 ± 0.04) compared with those of the untreated animals (0.50 ± 0.04; $P < 0.05$). This effect was more pronounced for regions with low NAA values (0.16 ± 0.03) that changed to 0.32 ± 0.03 ($P = 0.04$) for the treated group and to 0.10 ± 0.03 ($P = 0.20$) for the controls. DWI data showed better ischemic tissue condition for the treated rats, but the measured parameters showed only a trend of improvement. The MR results were corroborated by behavioral examinations.

Conclusion: Our findings suggest that SPG stimulation may ameliorate MR tissue characteristics following t-MCAO even if treatment is started 18 h post-occlusion.

Key Words: Sphenopalatine ganglion (SPG); middle cerebral artery occlusion (MCAO); N-acetyl aspartate (NAA); MRI; MR spectroscopy (MRS)
J. Magn. Reson. Imaging 2010;31:1355–1363.

STROKE IS A major cause for disability, death, and healthcare expenditure. It is the second most common cause of death worldwide, exceeded only by heart disease and the third most common cause for death in the United States (1,2). Ischemic stroke constitutes 83% to 90% of stroke cases in Western countries (1,3). The middle cerebral artery (MCA) in the anterior circulation, or its branches, is the most common site of occlusion, accounting for approximately 90% of infarcts and two-thirds of all strokes (4).

To date, treatments for acute ischemic stroke are limited and include intravenous recombinant tissue plasminogen activator (IV t-PA) and mechanical revascularization using thrombectomy devices, such as the MERCI device (5). However, in the United States, only approximately 3% of ischemic stroke patients are treated with IV t-PA mainly due to the short treatment window of only 3 and 8 h for IV t-PA and for MERCI device, respectively (6).

Due to the limited access to existing approved therapies as well as the related safety issues, there remains a pressing need for development of additional therapies for the treatment of acute ischemic stroke with a longer therapeutic window, as well as a need for an improvement in outcome during the rehabilitation phase. In the acute phase, the therapeutic focus is in limiting the ischemic insult by restoring or increasing cerebral blood flow (CBF). However, in the chronic phase other factors may affect tissue outcome (7).

The sphenopalatine ganglion (SPG) is the source of parasympathetic innervations to the anterior cerebral circulation, which comprises the middle cerebral artery, the anterior cerebral artery and their tributaries (8,9). Studies in rodents, dogs, and monkeys have demonstrated that stimulation of SPG neurons leads to a profound ipsilateral increase in the CBF as a result of arterial vasodilatation, and that the latter leads, in turn, to augmentation of tissue perfusion (8–10). Moreover, previous studies, including histopathologic studies in humans (11), have revealed that

School of Chemistry, The Raymond and Beverly Sackler Faculty of Exact Sciences, Tel Aviv University, Tel Aviv, Israel.

†*Dr. Nossin-Manor's present address is:* Diagnostic Imaging, The Hospital for Sick Children, Toronto, ON, Canada.

*Address reprint requests to: Y.C., School of Chemistry, The Raymond and Beverly Sackler Faculty of Exact Sciences, Tel Aviv University, Ramat Aviv, Tel Aviv 69978, Israel. E-mail: ycohen@post.tau.ac.il

Received July 20, 2009; Accepted January 6, 2010.
DOI 10.1002/jmri.22110
Published online in Wiley InterScience (www.interscience.wiley.com).

the main neurotransmitters of this neuronal pathway are acetyl choline (ACh), vasoactive intestinal peptide (VIP), and nitric oxide (NO) (12,13). It is interesting to note that NO is best known for its potent vasodilatory activity and its capacity for neuroprotection and neurogenesis. Several studies have demonstrated that the cerebral vasodilatation induced by SPG stimulation is indeed mediated through NO mechanisms (8) and that ablation of the SPG efferents to the cerebral vasculature leads to an increased infract size in MCA-occluded rats (14,15).

Recently, Henninger and Fisher (16) showed that SPG stimulation during the hyperacute phase of permanent middle cerebral artery occlusion (MCAO) in rats, had beneficial effect on perfusion and diffusion MRI parameters. Therefore, it is interesting to test whether SPG stimulation can prolong the window of treatment for stroke, and as such serve as a potential treatment.

MRI and MR spectroscopy (MRS) are widely used for investigating, in vivo, neurological disorders in general, and ischemic stroke in particular (17–19). The versatility of the MR technique enables noninvasive studying of not only the progression of neurological pathology during longitudinal follow-up, but also the evaluation of the pathophysiologic state of the studied tissue, without the need of animal sacrificing. Among the available MR approaches, diffusion weighted imaging (DWI) was found to be a powerful tool for early stroke detection, as first described by Moseley and coworkers (17). DWI enables observation of ischemic tissues within minutes following the ischemic event. Apparent diffusion coefficient (ADC) maps, calculated from DWI, may be used to evaluate infarct size as well as tissue condition, and were found to correlate with infarct sizes evaluated from histology (20,21). The acute stage of the ischemic stroke is characterized, *inter alia*, by cellular swelling (cytotoxic edema) and increase in the extracellular tortuosity that reduces the ADC of the water molecules in the ischemic region (17,18). In the chronic stage of ischemic stroke, high ADC values (compared with the contralateral regions) are observed for the infarct area as a result of the necrotic process that includes cells death and membrane loss (22). Therefore, computed ADC values in the ischemic hemisphere normalized to averaged ADC values of the contralateral hemisphere values, i.e., $(I/C)ADC_{av}$, may predict tissue condition (23,24). Simultaneously to the changes in the diffusion characteristics of water within the ischemic region, changes in levels of different brain metabolites can be detected by different MRS methodologies (25,26). Among these metabolites, N-acetyl-aspartate (NAA) is considered to be a marker for neuronal density and viability (27,28) affording information about the neuronal tissue condition and was claimed to predict the brain status at the chronic stage (29–31). A significant decrease in NAA levels was found few hours after ischemic stroke both in humans and animal-models. Therefore this metabolite is considered to be an indicator of brain tissue condition after an ischemic event.

The present study examines, in vivo, the effect of SPG stimulation that was started 18 ± 2 h after MCAO, on rat brain after 2 h of transient MCAO (t-MCAO) in three experimental time points. MRS and MRI measurements were performed 16 ± 2 h, 8 days, and 28 days, after MCAO. Rats were examined by ^{1}H-MRS imaging (^{1}H-MRSI), DWI and a modified neurological severity score (mNSS). NAA levels, as obtained from ^{1}H-MRSI, lesion volume (LV), and $(I/C)ADC_{av}$, were used to determine the pathophysiologic state of the control and SPG-treated groups.

MATERIALS AND METHODS

Surgical Protocols

The animal experiments have all been approved by animal care and use committee of Tel Aviv University. Male Wistar rats weighing 290 ± 10 g were used in the present study.

Electrode Implantation

Twenty-four hours before the MCAO procedure, the head skin of the rat was clipped and cut along the midline (craniocaudal axis). The skin and the orbital structures of the right side (ipsilateral to subsequent t-MCAO) were retracted laterally to expose the ethmoidal foramen and the ethmoidal nerve (i.e., the postganglionic parasympathetic nerve fibers from the SPG). A hook stimulating electrode, that was used to generate the electrical pulses, was then hooked onto the exposed fibers (8). The wire of the electrode was glued onto the skull, and the receiver was placed under the skin on the nape of the animal. The surgical wound was closed above the right orbit. All rats were implanted.

t-MCAO Procedure

Twenty-five rats were anesthetized with isoflurane (4% for induction, 2% for surgery) and ventilated with N_2O:O_2 (70:30%) mixture. Transient focal cerebral ischemia was induced by intraluminal suture occlusion of the right MCA, using the suture model as previously described (32). In brief, 4-0 monofilament nylon suture (SMI, Belgium) was coated with silicon (Wacker-Chemie, Germany) and inserted through the proximal external carotid artery into the internal carotid artery and then into the circle of Willis, effectively occluding the MCA. The suture was placed for 2 h and subsequently removed. The surgical wound was closed, and the animals returned to their cages for a recovery period of approximately 16 h.

Arterial blood samples were taken before, and immediately after the MCAO, to measure pH, PaO_2 and $PaCO_2$ (Table 1). Body temperature was maintained at 37.0 ± 0.5°C, using electrical heating pad.

From the 25 t-MCAO rats, 6 died during the first 16 h, before the first MR experiment. The remaining 19 rats were divided, arbitrary, to two groups: 11 rats at the control group and 8 rats at the treated group. Of the 11 rats from the control group, 4 died within the first week, and only 7 were finally included in the untreated group. In the stimulated groups (eight rats), two rats were taken out from the study due to

Table 1
Physiological Parameters Observed Before During and After the MCAO

	pCO_2 mmHg	pO_2 mmHg	pH
Before t-MCAO	33.4±3.4	123±26	7.42±0.04
After 1h MCAO	38.0±7.0	127±13	7.41±0.06
After 2h t-MCAO	30.6±1.3	132±37	7.44±0.03

technical problems of the stimulating electrode that appeared during the first week after the ischemic stroke. Therefore, only six rats of the SPG-treated rats completed the 28-day protocol.

MRI and MRS Protocols

MR experiments were performed using a 7T/30cm BioSpec system (Bruker, Germany) equipped with a BGU20 gradient system, capable of producing pulse gradients of 400mT/m in each of the three directions. A transmit body coil (ID = 150 mm) and receive surface coil (ID = 15 mm) actively decoupled were used to acquire the MRI and MRS data. Control (n = 7) and treated (n = 6) rats were examined by MRI and MRS under isoflurane anesthesia (induction 4.0%, maintenance 1.5%) in 70:30 N_2O:O_2 gas mixture. Each rat was examined at three time points: 16 ± 2 h, 8 days and 28 days after the t-MCAO.

MRI

T_2 weighted images (T_2WI) were collected using the RARE sequence (RARE factor=8) with the following parameters: field of view (FOV) of 2.56 × 2.56 cm^2 and 256 × 128 digital resolution reconstructed to 256 × 256. Eight continuous 2-mm slices were collected, using repetition time/echo time (TR/TE) of 3000/75 ms with four averages in 3 min 45 s. ADC maps were calculated from two spin-echo four-shot echo planar images (EPI), collected with and without diffusion sensitizing gradient pulses and with the following parameters: $\delta = 4.5$ ms, $\Delta = 40$ ms and G = 173mT/m, resulting in a b_{max} of 1500s/mm^2. The same geometry (i.e., slices and FOV) used in T_2WI experiments was used in the DWI protocol. For diffusion images, the matrix was 96 × 96 reconstructed to 128 × 128 with TR/TE = 2000/53 ms. The entire DWI protocol was completed within 2 min.

^{1}H-MRSI

Two-millimeter slice-selected two-dimensional (2D) ^{1}H-MRSI was performed with the following parameters: FOV of 2.56 × 2.56 cm^2 with VAPOR water suppression, a matrix of 8 × 8 reconstructed to 16 × 16, resulting in 256 voxels of 1.6 × 1.6 × 2.0 mm^3. TR/TE=2000/135 ms were used with 32 averages. The total collection time of the ^{1}H-MRSI data was 47 min.

SPG Stimulation Protocol

After the completion of the first MR protocol (18 ± 2 h after the t-MCAO) the SPG-stimulated rats (treated group) were moved to a dedicated RF activation cage (BrainsGate, Israel) which enables wireless stimulation. The following electrical stimulation protocol was applied: Two 60-s-long pulses separated by 12 s off-time, applied every 15 min (8 pulses per hour). Each pulse was of 2 mA amplitude, 0.5 ms pulse width and 10 Hz frequency. SPG stimulation started 18 ± 2 h after t-MCAO surgery and was applied for 3 h, for seven consecutive days.

Data Analysis

Evaluation of Normalized NAA Value

The 2D ^{1}H-MRSI raw data were split into 256 individual NMR spectra. Fifteen spectra from the ipsilateral hemisphere and their respective contralateral spectra (depicted in Fig. 2a) were used to calculate normalized NAA values for each examined animal at all three time points, i.e., at 16 ± 2 h, 8 days, and 28 days post–t-MCAO. NAA integration values were determined by using the line fitting procedure of the MestRe-C software (33). The NAA integration values of the ipsilateral voxels were normalized to the NAA values obtained for the contralateral voxels, to determine the normalized

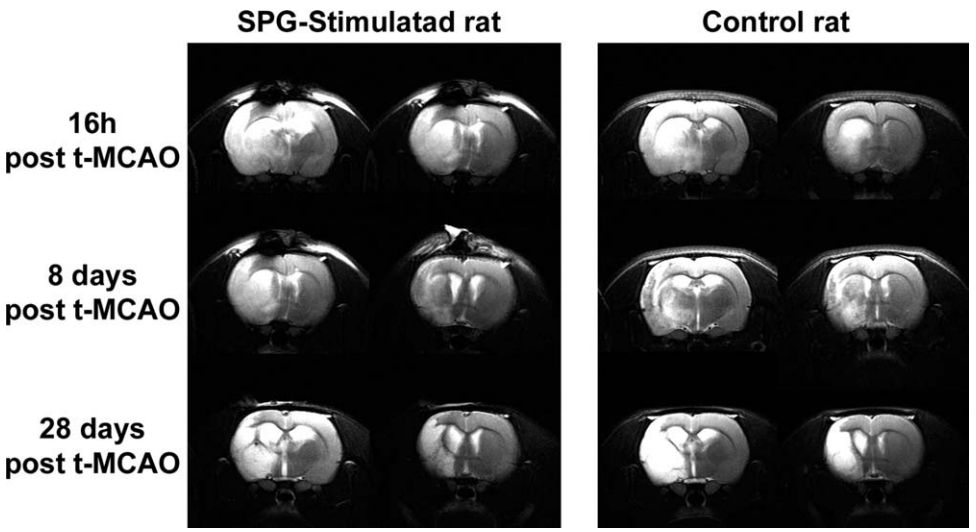

Figure 1. T2 weighted images of two continuous slices representing one ischemic rat from each examined group. Images were obtained 16 h, 8 days, and 28 days post–t-MCO.

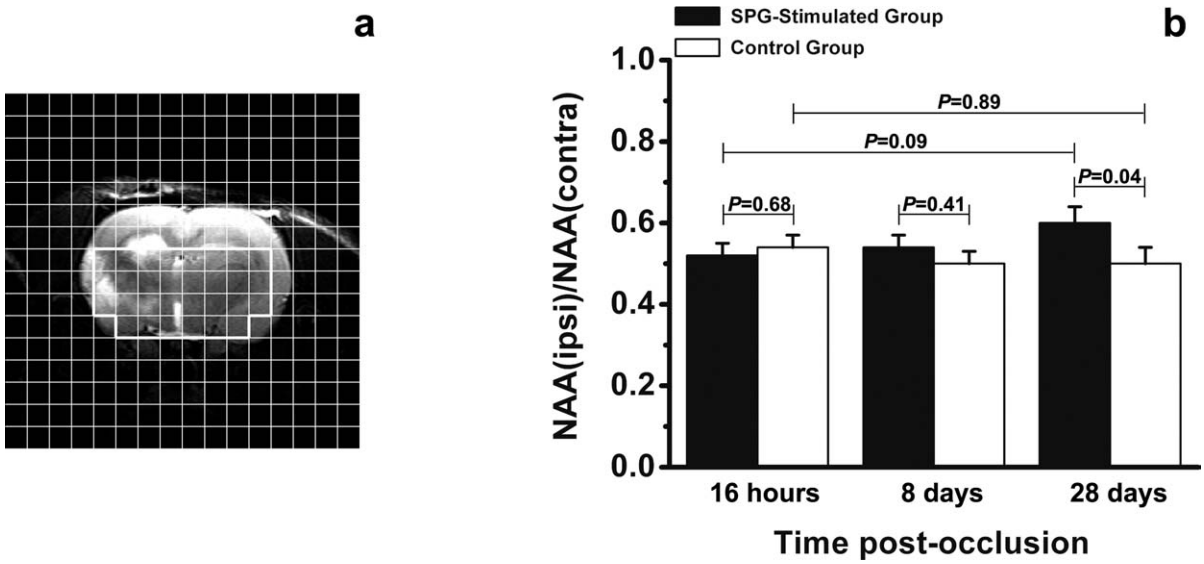

Figure 2. a: Representative ^{1}H-MRSI template placed on *T*2WI of rat brain acquired 16 h post–t-MCAO. The thick frame limits the voxels used for the NAA quantifications. **b**: Total normalized NAA values obtained from the examined rats at the three experimental time points, i.e., 16 ± 2 h, 8 days, and 28 days, after the t-MCAO. Black and white columns represent the averaged total normalized NAA values obtained for the SPG-stimulated and control rats, respectively.

level of the NAA in the ischemic side compared with the nonischemic side.

To gain more specific information on the changes in the normalized NAA values, we classified the normalized NAA values in the ischemic hemisphere, at the first experimental time point (before treatment), into three categories: (a) voxels with normalized NAA values greater than 0.7, (b) voxels with normalized-NAA values between 0.4 and 0.7, (c) voxels with normalized NAA values smaller than 0.4.

DWI Characteristics

All calculations were performed using an in-house MatLab® program. ADC maps were calculated from two contiguous EPI diffusion experiments with b-values of 1.5 and 1500 s/mm^2.

Lesion Volume

The lesion volume (LV) in percentages was calculated, blindly, for all slices. The area of DWI abnormality in each slice was determined visually and processed by an in-house Matlab® program. The lesion volume was obtained by multiplying the area obtained from the program by the slice thickness and dividing it by the brain volume. Sixteen hours after the t-MCAO, regions with lower ADC values compared with the contralateral hemisphere, were analyzed. Twenty-eight days after the t-MCAO, regions with higher ADC values compared with the contralateral hemisphere values, were chosen for the LV calculation.

(I/C)ADC$_{av}$

As suggested previously (23,24) hemispheric averaged ADC ratios (ipsilateral/contralateral [I/C]), i.e., (I/C)ADC$_{av}$, were calculated by dividing the average ADC value in the lesion area by the average ADC value of its respective contralateral region of interest (ROI):

$$(I/C)ADC_{av} = \frac{Average(ADC)_{ipsi-lateral}}{Average(ADC)_{contra-lateral}}$$

Behavioral Tests

A neurological mNSS test, scale 0–18, was performed (34) at day 1 before the first SPG stimulation session, at day 8 after last SPG stimulation session and at day 28.

Statistical Analysis

MRS and MRI results were analyzed by two-tailed Student's t-test. In the behavioral examinations (mNSS), one-way analysis of variance test was used to evaluate the significance of the results. $P < 0.05$ was considered significant.

RESULTS

Physiological Parameters

All rats involved in the study had normal physiological parameters, i.e., pH, pO_2, pCO_2 (Table 1) and temperature (maintained at 37.5°C by electrical heating pad), before, during, and after the occlusion procedure.

Figure 1 shows T_2 weighted images (T_2WIs) of one representative rat of each group. These images, which depict two continuous slices, demonstrate the ischemic region at the three studied time points, i.e., 16 h, 8 days, and 28 days after the stroke onset. As expected, T_2 hyperintensity is clearly observed 16 h, 8 days, and 28 days post-occlusion.

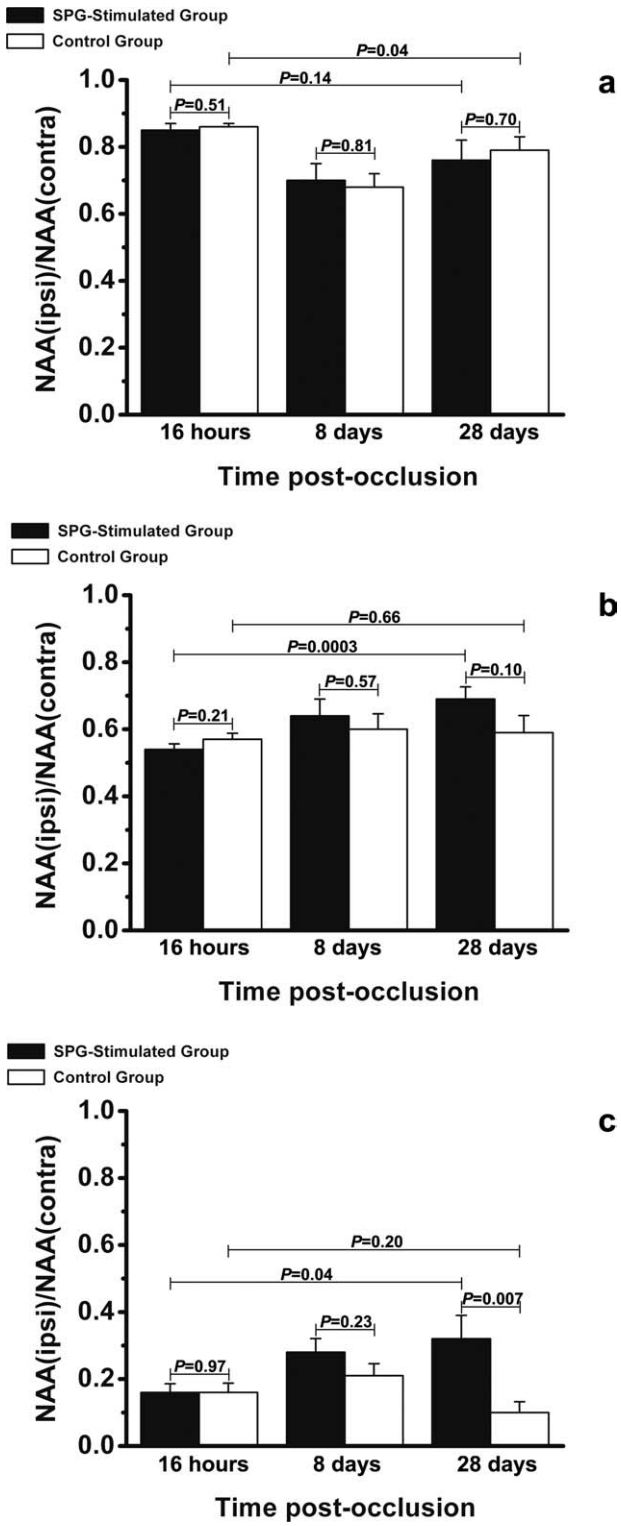

Figure 3. **a**: Temporal changes in normalized NAA values from voxels with normalized NAA values > 0.7 at 16 ± 2 h post–t-MCAO. **b**: Temporal changes in normalized NAA values at voxels with 0.4< normalized NAA values < 0.7 at 16 ± 2 h post–t-MCAO. **c**: Temporal changes in normalized NAA values at voxels with normalized NAA values < 0.4 at 16 ± 2 h post–t-MCAO. Black and white columns represent the total normalized NAA values obtained for the SPG-stimulated and control rats, respectively.

NAA level from ^{1}H-MRSI

Figure 2a schematically shows the template of the voxels of the 2D-^{1}H-MRSI experiments used to determine the NAA level in each examined animal. Figure 2b depicts the changes in the averaged total normalized NAA values for the three experimental time points after the t-MCAO for the two groups. This Figure clearly shows that there was a significant difference between the total averaged NAA values of the two groups at the end of the study (day 28), whereas such a difference was not observed at the first time point, i.e., 16 ± 2 h after the t-MCAO. The stimulated and control groups started from very similar averaged values of total normalized NAA values of 0.52 ± 0.03 and 0.54 ± 0.03, respectively ($P \asymp 0.7$), and reached different averaged normalized NAA values of 0.60 ± 0.04 and 0.50 ± 0.04, respectively, 28 days after the t-MCAO ($P < 0.05$).

To obtain more specific information from the MRS data, we classified the normalized NAA values in the ischemic hemisphere at 16 ± 2 h post–t-MCAO into three categories: (a) voxels with normalized NAA values greater than 0.7, (b) voxels with normalized NAA values between 0.4 and 0.7, and (c) voxels with normalized NAA values smaller than 0.4. The changes in the NAA values of each category are presented in Figure 3a–c. Figure 3a shows that there are no significant differences between SPG-stimulated and control groups at all three time points for voxels with normalized NAA values greater than 0.7. However, significant deterioration ($P = 0.04$) in the normalized NAA values of this category (category a) is observed for the untreated control rats at day 28 post-occlusion compared with the first time point. Figure 3b summarizes the changes in the averages of the normalized NAA values of voxels having initial normalized-NAA values greater than 0.4 and smaller than 0.7 (category b). In this case, we found highly significant increase ($P < 0.0005$) in normalized NAA values in the SPG-stimulated group compared with the control group, where such improvement in the normalized NAA was not observed. For these voxels, the normalized NAA values of the SPG-stimulated group increased from 0.54 ± 0.02 (16 ± 2 h) to 0.64 ± 0.05 (day 8) and then to 0.69 ± 0.04 (day 28, $P = 0.0003$), while those of the controls did not change significantly (from 0.57 ± 0.04 at 16 ± 2 h to 0.59 ± 0.05 28 days post–t-MCAO, $P = 0.66$). The most interesting results were found for voxels in which normalized NAA values were smaller than 0.4 at 16 ± 2 h post-occlusion (category c), as shown in Figure 3c. These voxels, which showed the most dramatic reduction in NAA levels 16 ± 2 h post-occlusion, also exhibited the most dramatic response to treatment. For these voxels, the control group showed a trend of deterioration in the normalized-NAA levels. However, this deterioration was not statistically significant. In the SPG-stimulated animals, NAA levels from these voxels significantly improved from 0.16 ± 0.03 at 16 ± 2 h to 0.32 ± 0.07 at 28 days post-MCAO ($P < 0.01$). For these voxels of category c, we found that although the control and SPG-stimulated groups had the same initial NAA

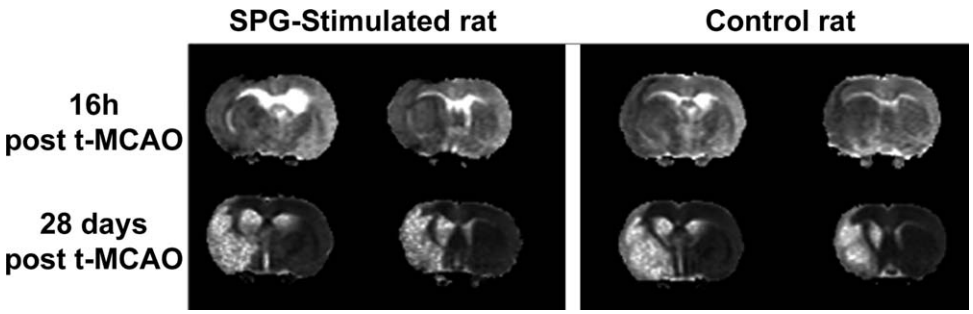

Figure 4. ADC maps calculated from the DWI data of two continuous slices representing one ischemic rat from each group. Images were obtained 16 h and 28 days post–t-MCO.

values at 16 ± 2 h post-occlusion (0.16 ± 0.03, $P = 0.97$), 28 days post-occlusion a dramatic difference in the normalized NAA values of the SPG-stimulated animals (0.32 ± 0.07) and the controls (0.10 ± 0.03, $P = 0.007$) was found.

ADC maps Analysis

Figure 4 shows ADC maps, calculated from the DWI experiments 16 h and 28 days post-occlusion. This figure shows the same slices depicted in Figure 1 and showed the contrast characteristics expected for ischemic brain (18). Sixteen hours post–t-MCAO the ADC values of the ischemic regions are lower as compared to the contralateral hemisphere. Twenty-eight days post-occlusion the ADC values of the ischemic region are, indeed, higher as compared to that of the contralateral hemisphere.

Figure 5a,b shows the percentage LV and the (I/C)ADC_{av} values, respectively, as calculated from the ADC maps. Both LV and (I/C)ADC_{av} were calculated for the treated and untreated groups 16 ± 2 h and 28 days post-occlusion and were not calculated for day 8 time point due to the pseudo normalization that occur at this time point (18,21). Of interest, for both investigated indices (Fig. 5a,b), very similar values were found 16 ± 2 h after the t-MCAO for both groups; however, less abnormal MRI indices were found for the stimulated rats 28 days post-occlusion. Figure 5a shows that both groups started with very similar LV, i.e., 21.1 ± 3.5% and 20.1 ± 4.5% for the controls and SPG-stimulated group, respectively ($P = 0.88$). Twenty-eight days post-occlusion, the LV of the treated rats decreased to 12.9 ± 3.1% ($P = 0.05$) while the LV of the controls decreased only to 15.6 ± 3.4% ($P = 0.05$). Despite that the difference between the LV values of the two groups at day 28 post-MCAO was not statistically significant ($P = 0.57$). More pronounced difference was observed when we examined the (I/C)ADC_{av} of the two groups as shown in Figure 5b. In this case, again, both groups gave the same value at 16 ± 2 h post-occlusion, 0.77 ± 0.02 for the controls and 0.75 ± 0.02 for the SPG-stimulated rats ($P = 0.52$). However, (I/C)ADC_{av} value of the controls was clearly higher as compared to the treated rats (2.22 ± 0.11 and 1.92 ± 0.14, respectively, $P = 0.13$). Although statistical differences were not observed in the parameters extracted from the diffusion MRI data, a trend of improvement in the tissue condition was observed for the SPG-treated group compared with the control group. This was found for the two DWI indices examined.

Modified Neurological Severity Score

Figure 6 shows the average mNSS values obtained for the two studied groups, at all three experimental time points. It should be noted that both groups started

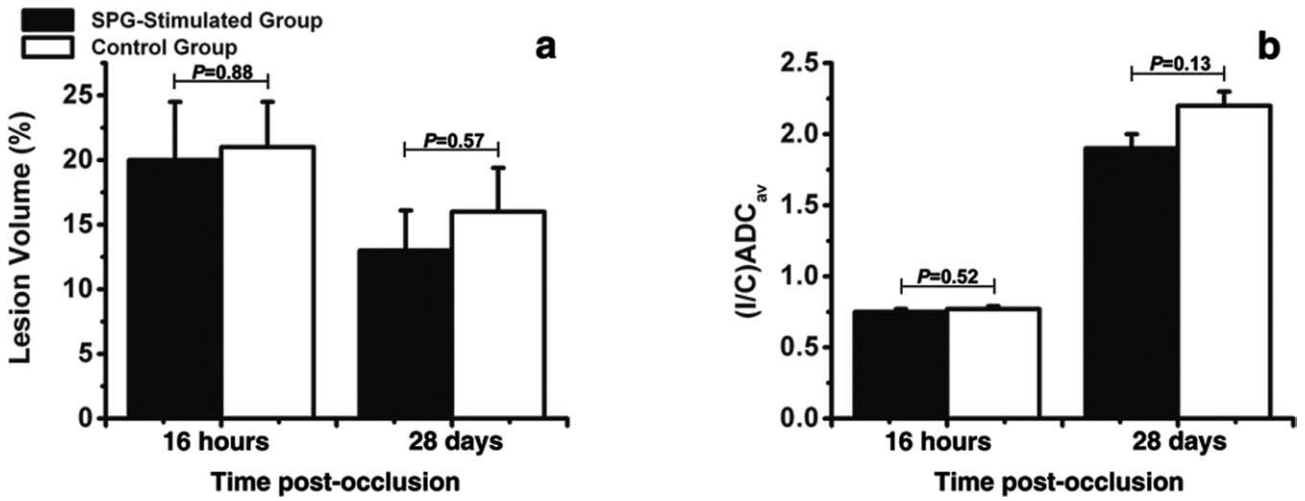

Figure 5. Changes in percent lesion volume (LV) (**a**) and in (I/C)ADC_{av} values (**b**) calculated from ADC maps obtained at 16 ± 2 h after the t-MCAO and 28 days post–t-MCAO. Black and white columns represent the LV and (I/C)ADC_{av} values obtained for the SPG-stimulated and control rats, respectively.

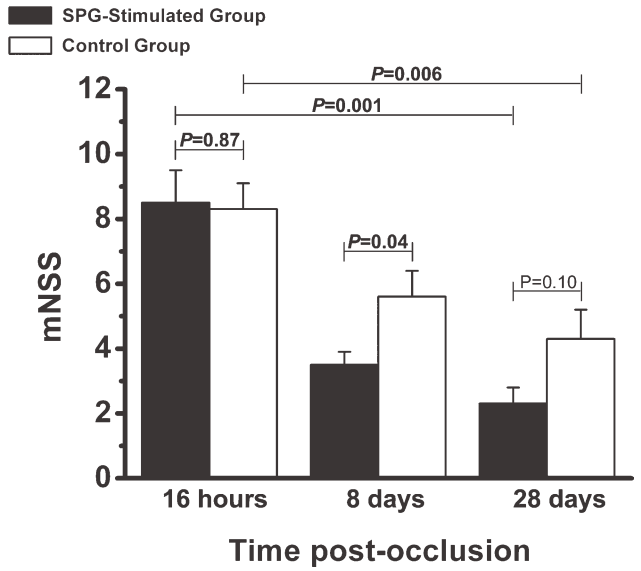

Figure 6. Temporal changes in the mNSS obtained at the three experimental time points: 16 ± 2 h, 8 days, and 28 days, post–t-MCAO. Black and white columns represent the mNSS values obtained for the SPG-stimulated and control rats, respectively.

from the same neuronal score with mNSS values of 8.5 ± 1.0 (for the SPG-stimulated group) and 8.3 ± 0.8 (for the control group, $P = 0.87$). Eight days after the t-MCAO, a significant difference in the mNSS of the two groups was found (5.6 ± 0.8 for the control rats and 3.8 ± 0.4 for the SPG-treated animals, $P = 0.04$). Twenty-eight days after the t-MCAO, the difference in the mNSS score between the groups was maintained (4.3 ± 0.9 versus 2.3 ± 0.5), however, it failed to reach statistical difference ($P = 0.10$).

DISCUSSION

In the present study we have examined, for the first time, the effect of SPG stimulation on the outcome following 2 h of t-MCAO in rats where treatment was started 18 ± 2 h after the occlusion. We used both MRS and MRI methods to test the temporal changes in the NAA values in the ischemic hemisphere and the DWI characteristics of the lesion areas, respectively, at 16 ± 2 h, 8 days and up to 28 days post-occlusion. MR data were compared with behavioral tests.

The main findings of this study are as follows: 1) the averaged total normalized NAA levels in the ischemic hemisphere show a more pronounced recovery in the SPG-treated animals 28 days post-MCAO. 2) This recovery is more significant in voxels with low initial normalized NAA levels. 3) Some differences in LV and (I/C)ADC_{av} values, which are not statistically significant, were observed between the groups at day 28, although both treated and untreated rats showed the same DWI characteristics 16 ± 2 h post-occlusion. 4) The mNSS values were also better for the SPG-treated rats, compared with controls although on day 28 post-MCAO the difference failed to reach statistical significance.

Of interest, we found that after SPG stimulation, the recovery in total NAA levels in the treated group was more pronounced compared with the controls. This effect was more pronounced in ROIs, where normalized NAA levels were initially more dramatically reduced. NAA concentrations in the brain are high and it is mainly localized to neurons (35); therefore, it has been considered as a neuronal marker (36). Reduction of NAA was often ascribed to neuronal loss but today it is clear that alternative explanations should be considered, as recovery in NAA was reported.

NAA recovery after cerebral ischemia was discussed previously in the literature (37) and the following possible contributions for this observation were suggested (38): (i) Surviving neuronal cells in the infarct area renew their ability to synthesize NAA, (ii) different cells start to express NAA, (iii) production of NAA from N-acetylaspartylglutamate (NAAG) by glial cells that are present in the infarct core, and (iv) neurogenesis, following the ischemic event.

In our study, the most reasonable explanation for the increase in the NAA levels in the stimulated group compared with the control group seems to be the renewal of the NAA synthesis by surviving neuronal cells. As shown previously, electrical stimulation of the SPG increases CBF in the infarct region (16). Because of the dependence of NAA synthesis on the energy levels in the cells (38,39), such a synthesis is reduced immediately after the ischemic event and the depletion of energy storage. Therefore, one can assume that the increase in NAA levels in the affected area may originate from the slow increase in the energy storage in these affected areas, which accumulated slowly as a result of the increase in the CBF occurring by the electrical stimulation of the SPG. Although the mechanism for this observation is not clear, this is an important result, in view of the fact that no NAA recovery had been found after tPA treatment (40).

Our DWI findings showed the same trend as the results obtained from the comparison of the NAA levels of the two studied groups. Like in the spectroscopic data, both groups had very similar baseline diffusion characteristics, and similar LV and (I/C)ADC_{av} values were computed 16 ± 2 h post-MCAO, i.e., before starting the treatment. Interestingly, according to the diffusion data, the treated group had a smaller LV value 28 days post-occlusion as compared to the control group, but this difference was not statistically significant. A more pronounced difference between the two groups was found in the (I/C)ADC_{av} index, where (I/C)ADC_{av} of the controls, at day 28, was higher as compared to the SPG-treated rats. In this case, a clear trend was observed but the difference was not statistically significant ($P = 0.13$). These results seem to indicate that the cytoarchitecture destruction in the controls is more severe as compare to the treated rats (21).

With regard to behavioral tests, we found significantly better mNSS in the treated group 8 days after t-MCAO. This difference did not reach statistical significant level at 28 days.

The improvements computed from the MR data and from the behavioral tests are even more dramatic because 4 (of 11) rats of the control group that received no treatment died while no such mortality was not observed for the SPG-treated group.

It has been recently shown that SPG stimulation affects perfusion and diffusion MRI parameters; however, in that study, only the hyperacute stage was examined in a model of permanent MCAO (16), and treatment started 60 min after the induction of stroke. However, in our study, significant improvement in NAA level and a clear trend of improvement in the DWI and behavioral parameters were found, despite the fact that treatment was started 18 ± 2 h post-MCAO. In addition no mortality was found in the treated group compared with a 36% mortality in the control group making the result even more significant.

In conclusion, this study shows that SPG-stimulation treatment of rats after 2 h of t-MCAO that was started 18 ± 2 h after the induction of stroke improve NAA levels and DWI characteristics in the ischemic hemisphere of the treated rats 28 days after t-MCAO. Our results, which were corroborated by behavioral examinations, demonstrate significant improvement in the normalized NAA values. This result was most pronounced at regions where the NAA levels were most decreased. The fact that treatment was started 18 ± 2 h after the ischemic event shows that this unique treatment of the electrical stimulation of the SPG can potentially extend the therapeutic window for the treatment of ischemic stroke.

ACKNOWLEDGMENTS

The MRI scanner used was purchased with grants from the Israel Science Foundation (ISF), and the Raymond and Beverly Sackler Center for Biophysics of Tel Aviv University. We thank the Alfredo Federico Strauss Center for Computational NeuroImaging of Tel Aviv University. This study was partly funded by BrainsGate LTD.

REFERENCES

1. American Heart Association: Heart disease and stroke statistics - 2005 update. Dallas, Texas: American Heart Association; 2005.
2. Murray CJL, Lopez AD. Mortality by cause for eight regions of the world: global burden of disease study. Lancet 1997;349: 1269–1276.
3. Feigin VL, Lawes CMM, Bennett DA, Anderson CS. Stroke epidemiology: a review of population-based studies of incidence, prevalence, and case-fatality in the late 20th century. Lancet Neurol 2003;2:43–53.
4. Moustafa RR, Baron JC. Clinical review: imaging in ischaemic stroke - implications for acute management. Crit Care 2007;11: 1–9.
5. Fisher M, Bastan B. Treating acute ischemic stroke. Curr Opin Drug Discov Devel 2008;11:626–632.
6. Smith WS, Sung G, Starkman S, et al. Safety and efficacy of mechanical embolectomy in acute ischemic stroke- results of the MERCI trial. Stroke 2005;36:1432–1438.
7. Cramer SC, Koroshetz WJ, Finklestein SP. The case for modality-specific outcome measures in clinical trials of stroke recovery-promoting agents. Stroke 2007;38:1393–1395.
8. Ayajiki K, Fujioka H, Shinozaki K, Okamura T. Effects of capsaicin and nitric oxide synthase inhibitor on increase in cerebral blood flow induced by sensory and parasympathetic nerve stimulation in the rat. J Appl Physiol 2005;98:1792–1798.
9. Suzuki N, Hardebo JE, Kahrstrom J, Owman C. Selective electrical-stimulation of postganglionic cerebrovascular parasympathetic nerve fibers originating from the Sphenopalatine Ganglion enhances cortical blood-flow in the rat. J Cereb Blood Flow Metab 1990;10:383–391.
10. Yarnitsky D, Lorian A, Shalev A, et al. Reversal of cerebral vasospasm by sphenopalatine ganglion stimulation in a dog model of subarachnoid hemorrhage. Surg Neurol 2005;64:5–11.
11. Uddman R, Tajti J, Moller S, Sundler F, Edvinsson L. Neuronal messengers and peptide receptors in the human sphenopalatine and otic ganglia. Brain Res 1999;826:193–199.
12. Suzuki N, Hardebo JE, Kahrstrom J, Owman C. Neuropeptide-y coexists with vasoactive intestinal polypeptide and acetylcholine in parasympathetic cerebrovascular nerves originating in the sphenopalatine, otic, and internal carotid ganglia of the rat. Neuroscience 1990;36:507–519.
13. Suzuki N, Hardebo JE. The cerebrovascular parasympathetic innervation. Cerebrovasc Brain Metab Rev 1993;5:33–46.
14. Kano M, Moskowitz MA, Yokota M. Parasympathetic denervation of rat pial vessels significantly increases infarction volume following middle cerebral artery occlusion. J Cereb Blood Flow Metab 1991;11:628–637.
15. Koketsu N, Moskowitz MA, Kontos HA, Yokota M, Shimizu T. Chronic parasympathetic sectioning decreases regional cerebral blood-flow during hemorrhagic hypotension and increases infarct size after middle cerebral-artery occlusion in spontaneously hypertensive rats. J Cereb Blood Flow Metab 1992;12: 613–620.
16. Henninger N, Fisher M. Stimulating circle of Willis nerve fibers preserves the diffusion-perfusion mismatch in experimental stroke. Stroke 2007;38:2779–2786.
17. Moseley ME, Cohen Y, Mintorovitch J, et al. Early detection of regional cerebral ischemia in cats- comparison of diffusion weighted and T2-weighted MRI and Spectroscopy. Magn Reson Med 1990;14:330–346.
18. Hoehn M, Nicolay K, Franke C, van der Sanden B. Application of magnetic resonance to animal models of cerebral ischemia. J Magn Reson Imaging 2001;14:491–509.
19. Mikulis DJ, Roberts TPL. Neuro MR: protocols. J Magn Reson Imaging 2007;26:838–847.
20. Back T. Hemmen T, Schuler OG. Lesion evolution in cerebral ischemia. J Neurol 2004;251:388–397.
21. Sotak CH. Nuclear magnetic resonance (NMR) measurement of the apparent diffusion coefficient (ADC) of tissue water and its relationship to cell volume changes in pathological states. Neurochem Int 2004;45:569–582.
22. Nagesh V, Welch KMA, Windham JP, et al. Time course of ADC(w) changes in ischemic stroke: beyond the human eye! Stroke 1998; 29:1778–1782.
23. Ulug AM, Beauchamp N, Bryan RN, van Zijl PCM. Absolute quantitation of diffusion constants in human stroke. Stroke 1997;28: 483–490.
24. Li FH, Han SS, Tatlisumak T, et al. Reversal of acute apparent diffusion coefficient abnormalities and delayed neuronal death following transient focal cerebral ischemia in rats. Ann Neurol 1999;46:333–342.
25. Wardlaw JM, Marshall I, Wild J, Dennis MS, Cannon J, Lewis SC. Studies of acute ischemic stroke with proton magnetic resonance spectroscopy - relation between time from onset, neurological deficit, metabolite abnormalities in the infarct, blood flow, and clinical outcome. Stroke 1998;29:1618–1624.
26. Igarashi H, Kwee IL, Nakada T, Katayama Y, Terashi A. ^{1}H magnetic resonance spectroscopic imaging of permanent focal cerebral ischemia in rat: longitudinal metabolic changes in ischemic core and rim. Brain Res 2001;907:208–221.
27. Demougeot C, Garnier P, Mossiat C, et al. N-Acetyl-aspartate, a marker of both cellular dysfunction and neuronal loss: its relevance to studies of acute brain injury. J Neurochem 2001;77: 408–415.
28. Demougeot C, Bertrand N, Prigent-Tessier A, et al. Reversible loss of N-acetyl-aspartate in rats subjected to long-term focal cerebral ischemia. J Cereb Blood Flow Metab 2003;23:482–489.
29. Kamada K, Houkin K, Iwasaki Y, Abe H, Kashiwaba T. Metabolic and neurological patterns in chronic cerebral infarction: a single-

voxel ^{1}H-MR spectroscopy study. Neuroradiology 1997;39: 560–565.
30. Parsons MW, Li T, Barber PA, et al. Combined 1H MR spectroscopy and diffusion-weighted MRI improves the prediction of stroke outcome. Neurology 2000;55:498–505.
31. Demougeot C, Marie C, Giroud M, Beley A. N-Acetyl-aspartate: a literature review of animal research on brain ischaemia. J Neurochem 2004;90:776–783.
32. Spratt NJ, Fernandez J, Chen M, et al. Modification of the method of thread manufacture improves stroke induction rate and reduces mortality after thread-occlusion of the middle cerebral artery in young or aged rats. J Neurosci Methods 2006;155: 285–290.
33. Cobas JC, Sardina FJ. Nuclear magnetic resonance data processing. MestRe-C: a software package for desktop computers. Concepts Magn Reson Part A 2003;19:80–96.
34. Chen JL, Li Y, Wang L, et al. Therapeutic benefit of intravenous administration of bone marrow stromal cells after cerebral ischemia in rats. Stroke 2001;32:1005–1011.
35. Moffett JR, Namboodiri MAA, Cangro CB, Neale JH. Immunohistochemical localization of N-Acetyl-aspartate in rat brain. Neuroreport 1991;2:131–134.
36. Bruhn H, Frahm J, Gyngell ML, Merboldt KD, Hanicke W, Sauter R. Cerebral metabolism in man after acute stroke - new observations using localized proton NMR-spectroscopy. Magn Reson Med 1989;9:126–131.
37. Sager TN, Laursen H, Hansen AJ. Changes in N-Acetyl-aspartate content during focal and global brain ischemia of the rat. J Cereb Blood Flow Metab 1995;15:639–646.
38. Moffett JR, Ross B, Arun P, Madhavarao CN, Namboodiri AMA. N-Acetyl-aspartate in the CNS: from neurodiagnostics to neurobiology. Prog Neurobiol 2007;81:89–131.
39. Clark JB. N-acetyl-aspartate: a marker for neuronal loss or mitochondrial dysfunction. Dev Neurosci 1998;20:271–276.
40. Franke C, Brinker G, Pillekamp F, Hoehn M. Probability of metabolic tissue recovery after thrombolytic treatment of experimental stroke: a magnetic resonance spectroscopic imaging study in rat brain. J Cereb Blood Flow Metab 2000;20:583–591.